Understanding protein-nanoparticle interactions leading to protein corona formation: In vitro - in vivo correlation study

Cintia Marques, Plinio Maroni, Lionel Maurizi, Olivier Jordan, Gerrit Borchard

Understanding Protein-Nanoparticle Interactions Leading to Protein Corona Formation: *In Vitro* - *In Vivo* Correlation Study

Cintia Marques [a,b], Plinio Maroni [c], Lionel Maurizi [d], Olivier Jordan [a,b] and Gerrit Borchard [a,b]

[a] Institute of Pharmaceutical Sciences of Western Switzerland, University of Geneva, 1 Rue Michel Servet, 1211 Geneva, Switzerland
[b] Section of Pharmaceutical Sciences, University of Geneva, 1 Rue Michel Servet, 1211 Geneva, Switzerland
[c] Department of Inorganic and Analytical Chemistry, University of Geneva, Faculty of Sciences, Quai Ernest-Ansermet 30, Geneva 4 1211, Switzerland
[d] Laboratoire Interdisciplinaire Carnot de Bourgogne (ICB), UMR 6303 CNRS—Université Bourgogne Franche-Comté, BP 47870, CEDEX, Dijon, France

Abstract

Nanoparticles (NPs) in contact with biological fluids form a biomolecular corona through interactions with proteins, lipids, and sugars, acquiring new physicochemical properties. This work explores the interaction between selected proteins (hemoglobin and fetuin-A) that may alter NP circulation time and NPs of different surface charges (neutral, positive, and negative). The interaction with key proteins albumin and transferrin, the two of the most abundant proteins in plasma was also studied. Binding affinity was investigated using quartz crystal microbalance and fluorescence quenching, while circular dichroism assessed potential conformational changes. The data obtained from *in vitro* experiments were compared to *in vivo* protein corona data. The results indicate that electrostatic interactions primarily drive protein-NP interactions, and higher binding affinity does not necessarily translate into more significant structural changes. *In vitro* and single protein-NP studies provide valuable insights that can be correlated with *in vivo* observations, opening exciting possibilities for future protein corona studies.

Keywords: nanoparticle; protein corona; protein structure; binding affinity; conformational changes

1. Introduction

When nanoparticles (NPs) come into contact with biological fluids, they interact with proteins, lipids, and sugars, forming a biomolecular corona on the NP surface. These interactions result in the development of a new "biological identity" for the nanoparticles, accompanied by the acquisition of new physicochemical properties [1-4].

Protein corona studies evolved over the last decade [5]. Initial experimental studies attempted to understand its mechanisms, which proved to be difficult. The focus shifted to trying to avoid protein corona formation by developing stealth NPs, and more recently, the efforts switched to exploiting key proteins to design the protein corona. Numerous *ex vivo*, *in vivo*, and *in vitro* studies have been carried out during this evolution. However, the comparison and translation between these studies are still challenging, mainly due to the lack of standardization [6].

Moreover, it is important to discuss the relevance and challenges of *in vivo vs. in vitro* correlation studies as well as single protein-NPs *vs.* all blood proteins-NPs interaction experiments. *In vivo*, the characteristics of the protein corona display a high complexity since they will be affected by the dynamic interactions between nanoparticles and various biological components (biological fluids, interaction with cells, different physiological flow, immune response, etc.). Similarly, *in vitro* blood proteins-NPs studies offer data that are supposedly closer to the physiological behavior than single protein-NPs studies. The most common studies consist of having a library of NPs of different physicochemical properties, which would be correlated to the protein corona composition, such as NP size [1, 7-9], morphology [3, 9-11], surface chemistry [10, 12], hydrophobicity [13, 14], and charge [8, 10, 13]). However, under physiological conditions, the variables are not only NP characteristics but protein corona can also be influenced by gender [14] and by health conditions [15, 16], adding an extra layer of complexity to the analysis and making it more difficult to connect protein corona patterns with NP properties. Thus *in vitro* and single protein-NPs studies are important to have better control over the different variables that influence protein corona formation and obtain direct results that can be correlated to *in vivo* studies. While the direct comparison between *in vivo* and *in vitro* data has limitations, integrating findings from both types of experiments can provide a comprehensive understanding of the protein corona phenomenon.

In a previous study, superparamagnetic iron oxide nanoparticles (SPIONs) coated with polyvinyl alcohol (PVAL) displaying either neutral ([0] NPs), positive (+ NPs), or negative (- NPs) surface charges were injected into the tail vein of rats, and the protein corona composition was tracked over time [17]. Depending on their surface chemistry/charge and resulting corona composition, NPs showed different retention times in blood circulation. Positively charged PVAL-SPIONs showed the shortest circulation time, which was attributed to high hemoglobin adsorption. Moreover, neutral NPs had the longest circulation time, which might be related to the presence of several proteins, such as alpha-2-HS-glycoprotein (fetuin-A).

This work explores the interaction between these previously identified key proteins and the PVAL-coated SPIONs, investigating binding affinity and structural changes of protein upon binding to NPs. Besides hemoglobin (Hb) and fetuin-A (Ft), albumin (BSA) and transferrin (Tf) interaction with NPs was studied, as well since they are two of the most abundant proteins in plasma. To do so, fluorescence quenching and quartz crystal microbalance (QCM) were used to determine binding affinity, while potential changes of the secondary protein structure were characterized by circular dichroism (CD). The results were compared to data previously published, obtained from *in vivo* experiments [17], in order to determine how simple protein-NP experiments can be correlated to the *in vivo* complexity of the protein corona.

2. Methods

Materials

Polyvinyl alcohol (PVAL-OH; Kuraray Poval 3-85) and carboxyl modified polyvinyl alcohol (PVAL-COOH; Kuraray Poval 3-86 SD) were supplied by Kuraray Co., Ltd. Polyvinyl/Vinyl amine copolymer (PVAL-NH_2; Selvol Ultiloc 5003) was supplied by Sekisui Chemical Co., LTD. BSA (66 kDA, A9647), holo-transferrin human (T0665), hemoglobin human (H7379), fetuin from fetal bovine serum (F3385) and phosphate buffered saline 10x (PBS) and other chemicals were purchased from Sigma-Aldrich (Buchs, Switzerland).

PVAL-SPIONs were produced according to Marques et al [18]. Hydrodynamic diameter (Dh), and zeta potential were measured by Dynamic Light Scattering (DLS) and Electrophoretic Light Scattering (ELS). The obtained NPs had the following characteristics in PBS 0.1x: PVAL-COOH SPIONs (hydrodynamic diameter (Dh) of 130 ± 2 nm, -13.1 ± 0.2 mV), PVAL-OH SPIONs (Dh 71 ± 4 nm, -4 ± 0.3 mV) and PVAL-NH_2 (Dh 81 ± 1 nm, +0.5 ± 0.3 mV) [18].

Preparation of Quartz Crystal Microbalance (QCM) sensor chips

Silica sensor ships (Q Sense E1/E4) were supplied from China by Renlux Tek Co., Limited. The sensors were initially cleaned with piranha solution for 15 min, which also increases OH availability. The wash was followed by an aminosilanization and glutaraldehyde treatment to functionalize the sensors with aldehyde groups, subsequently bound to proteins' positively charged amino acids (arginine, histidine and lysine).

For the aminosilanization step, sensors were immersed in acetone, followed by immersion in an aminosilane solution - (3-Aminopropyl)triethoxysilane 2 % v/v. The chips were dipped again in the acetone jar to remove excess, weakly physisorbed aminosilane and baked for 1 h at 110 °C. Then the sensors were sonicated for 10 min in ethanol, another 5 min in milliQ® water, rinsed briefly with milliQ® water and dried with nitrogen gas.

Finally, the sensors were placed in a “humidity chamber”, covered with 1 to 2 drops of 8 % glutaraldehyde solution, and incubated at room temperature for 30 min. Then sensors were washed with water and dried with nitrogen gas.

Nanoparticles’ binding studies with QCM

Q-sense E4 (Gothenburg, Sweden) with a flow-through cell was used to measure the change in mass on the sensor, and a peristaltic pump was used to pump solutions through the circular thin-layer cell, which features two eccentric holes as the inlet and outlet.

First, the sensors were cleaned with milliQ® water, followed by PBS 1x. Resonance frequency was monitored and when equilibrium was reached, in around 20 min, a protein solution of 0.05 mg/ml in PBS 1x (BSA, Tf, Hb or Ft) was applied until reaching equilibrium again. The protein mass on the sensor was calculated with the equation 1 [19]:

$$\frac{\Delta f}{n} = -\frac{\Delta m}{C} \leftrightarrow F = -\frac{\Delta m}{C} \leftrightarrow \Delta m = -F * C \quad \text{(Equation 1)}$$

Where Δm corresponds to the protein mass on the sensor, C= 17.7 ng Hz^{-1} m^{-2} is the mass sensitivity constant, and n is the overtone number (in this case n = 5).

Protein coated sensors were then washed with PBS 1x before applying the NPs solution (0.1 mg Fe/ml). Once NPs reached an equilibrium, the sensor was washed with PBS 1x to check for loose protein-NPs interaction. All measurements were made in triplicate, at 25 °C.

Fluorescence spectroscopy measurements

BSA, Tf and Ft 4 µM were incubated with increasing concentration of coated PVA-SPIONs (100 µM, 150 µM, 200 µM, 250 µM, 300 µM and 350 µM of Fe_2O_3), for 1h at 25 °C or 37 °C, with agitation (80 rpm). To ensure a good fluorescence signal, 6 µM of Hb were used, keeping the same protein/SPIONs ratio. All samples were formulated in PBS 1x (Sigma-Aldrich, Switzerland). Steady-state fluorescence measurements were performed on Synergy Mx multimode microplate reader (BioTek Instruments, Inc., USA), on a 96 well plate (150 ul of samples /well). The excitation wavelength was 295 nm (to excite tryptophan residue) [20], and the fluorescence emission was scanned from 320 to 500 nm, with a 2 nm step, at 25 °C and 37 °C.

To calculate the affinity constants, the intensity of fluorescence was considered at the maximum emission of fluorescence of each protein (BSA = 338 nm, Tf = 326 nm, BSA = 334 nm and Hb = 326 nm). To compare the quenching effect of coated SPIONs, the area under the curve (AUC) from each spectrum was plotted on a bar graph. All samples were measured in triplicates (n=3).

UV-visible absorption measurements

6 µM of Hb were incubated with 150 µM, 225 µM, 300 µM, 375 µM, 450 µM and 525 µM of PVA-coated SPIONs (concentration expressed in terms of of Fe_2O_3), for 1h at 25 °C, with agitation (80 rpm). All samples were solubilized in PBS 1x (Sigma-Aldrich, Switzerland). Uv-visible measurements were performed on Synergy Mx multimode microplate reader (BioTek Instruments, Inc., USA), on a 96 well plate (150 ul of samples /well). The absorption spectra were acquired from 230 nm to 700 nm, with a 10 nm step, at 25 °C.

Circular Dichroism

To study the protein's secondary structure while interacting with NPs of different charges, 0.4 µM of protein solution (BSA, Tf, Hb or Ft) was incubated with 80 µM of coated SPIONs, for 1h, at 37°C, with agitation. All solutions were prepared in milliQ® water. CD measurements were carried out at 25 °C using a spectro-polarimeter (JASCO J-810, Japan), with a 5 mm path length quartz cell. Spectra were recorded from 190 nm to 260 nm (far-UV region) with a 1nm bandwidth under a constant flow of nitrogen gas. Scanning speed was 20 nm/min and each spectrum resulted from 4 accumulations. Spectra were smoothed by applying the Savitzkx-Golay filter. The measurements were made in triplicates (n=3).
CD spectra were evaluated to estimate the proportions of secondary structure using the on-line DichroWeb server [21].

3. Results and discussion

3.1. Binding affinity

3.1.1. Quartz Crystal Microbalance

To study the interaction between NPs and proteins in a dynamic mode, we used a quartz microbalance to monitor the mass of NPs flowing above a protein-coated surface and able to bind to this surface (Figure 1a). Silica sensors were coated with the different proteins of interest - albumin, transferrin, hemoglobin, and fetuin. The coating process was monitored to ensure the sensor's total coverage, which is shown in Figure S1 and Table S1. It is important to note that the calculations consider that proteins are spherical, with the diameter corresponding to the longest dimension of the protein (Table S1 and Figure S2). While the shape of hemoglobin is close to spherical, that is not the case for the other proteins, which have a more ellipsoidal appearance. [22-24].

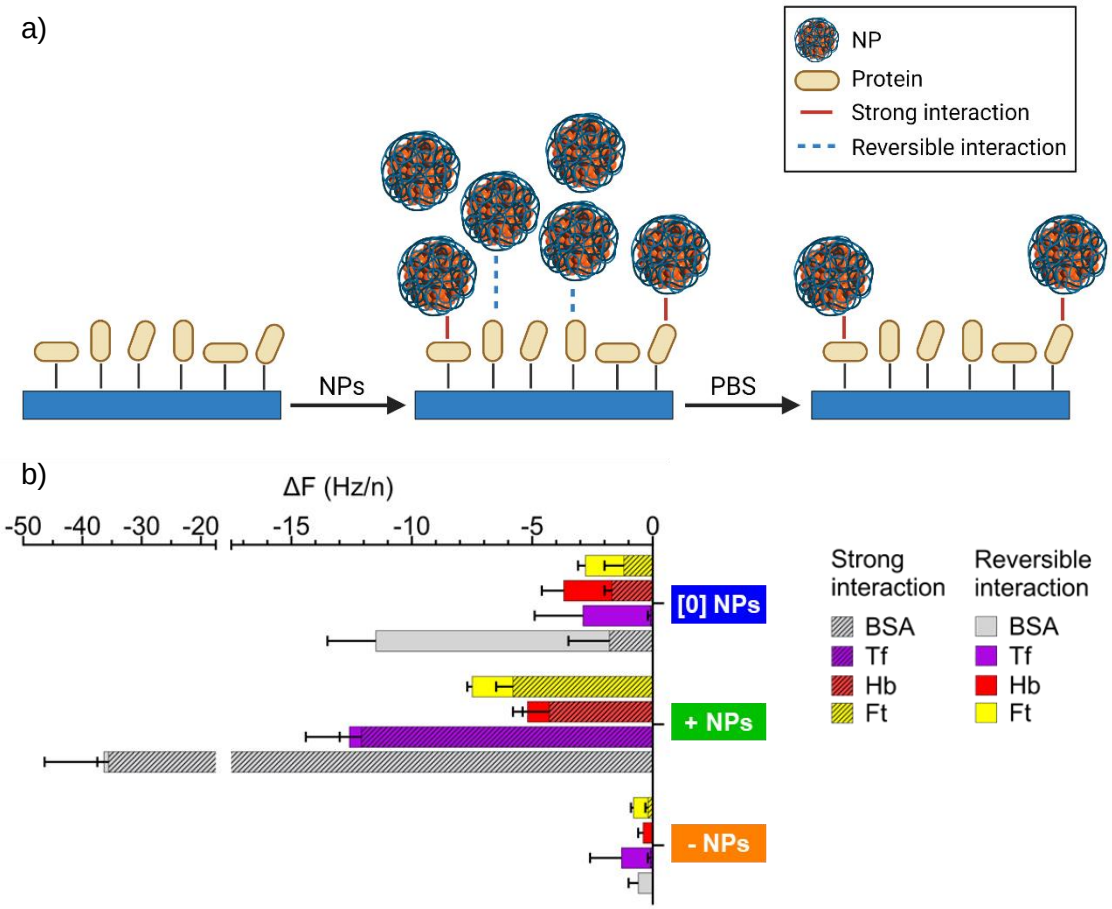

Figure 1. QCM scheme (a) represents the sensor coated with proteins and its interaction with the NPs. After the protein-NPs interaction reached an equilibrium, the sensor was washed with PBS. The NPs remaining attached to the sensor were classified as having established a "strong interaction" with the protein, while the NPs removed by the buffer were classified as establishing a "reversible interaction" with the proteins. The change in frequency derived from the interaction between the protein sensors and the NPs of different charges is presented in (b), where the solid color bar corresponds to a reversible interaction, and the cross-hatched bars indicates strong interaction.

Proteins should bind with a random orientation to the aldehyde functionalized QCM sensor (side on or end on), as considered in the calculations. It cannot be excluded that some orientations might be more favorable, meaning that the surface coverage (Figure S1) might be over- or underestimated. Moreover, QCM measures "wet" mass, since the measurement includes the water trapped in the film, which can also lead to an overestimation of the adsorbed amount. According to this simple model, transferrin and fetuin-A would tend to form a multilayer (with surface coverage > 100 %), while albumin and hemoglobin form a monolayer. Independently of the number of layers, the goal was to completely cover the surface to avoid unspecific interaction with the aldehyde functionalized QCM sensor. Since calculated hemoglobin coverage was

below 100 %, the NP adsorption profiles on the Hb sensor were compared with the NP adsorption on the aldehyde sensor (blank measurement) to rule out potential unspecific binding (Figure S3). Because aldehyde is negatively charged, it is expected to interact the most with the positively charged NPs (+ NPs), followed by the neutral [0] NPs. Figure S3 reveals that the affinity of + NPs and [0] NPs to the aldehyde sensor is about 10 and 6 times higher, respectively, than the NP interaction with the Hb-coated sensor. These results support full hemoglobin coverage of the sensor.

Once the full coverage of the sensor by proteins was ensured, we studied the interaction between the fixed proteins and the circulating NPs, which would pass over the sensor at a continuous flow. The change in mass on the sensor is summarized in Figure 1b, which shows that protein-NPs interactions resulted in a low change in frequency, suggesting low binding affinities due to the unspecific interaction between the NPs and the proteins.

To determine the binding affinity constant with QCM, it was necessary to increase the NP concentrations, which would increase the mass change on the sensor, allowing to build a binding isotherm curve. However, to obtain the results displayed in Figure 1b, the concentration of NPs was already high, making it technically impossible to quantify the binding affinity. Still, the data gives us a qualitative picture of the interactions between the NPs and the proteins.

Positively and negatively charged NPs had the highest and lowest interaction with the proteins, respectively (Figure 1b). Moreover, all proteins are negatively charged at pH 7.4 (excepted for the two alpha chains of the hemoglobin, Table S2). Thus, the results suggest that electrostatic interactions direct protein-NP interaction.

NPs interacted with the proteins in a continuous flow, and the maximum interaction was achieved once the mass adsorbed onto the sensor was stable (example in Figure S3a and b), then the sensor was cleaned with PBS, which often led to the partial removal of NPs from the sensor. The remaining NPs mass on the sensor after wash was considered to have a “strong interaction” with the proteins, while the mass of NPs washed away was classified as having a “reversible interaction” (Figure 1). Following this rationale, BSA had the highest interaction with NPs in general, but while its interaction with + NPs was mainly strong, albumin’s interaction with [0] NPs was mainly reversible. This tendency was followed by the other proteins since the interaction with + NPs was mainly irreversible, the interaction with [0] NPs was a mix between strong and reversible interactions, while interactions with – NPs were mainly reversible.

Furthermore, even though the protein were bound to the sensor, one can hypothesize that a “strong interaction” translates into a higher chance of the protein suffering structural changes *in vivo*, which might lead to the exposure of more epitopes, increasing the potential interaction with the NPs surface and with other proteins.

3.1.2. Fluorescence quenching (quantitative analysis)

Fluorescence quenching has been widely applied to study protein binding affinity and to predict potential structural changes [13, 20, 25-27]. Tryptophan moieties were selectively excited at 295 nm, so that a change in the polarity on the amino acid

microenvironment would lead to a shift in the maximum wavelength of emission (λ_{max}) [26, 28-31].

To define the protein/NPs ratios, we took the albumin/NPs ratio used in a previous *in vivo* experiment as reference [17], where 0.559 mg Fe/ml of coated SPIONs (corresponding to 5000 µM of Fe_2O_3, defined as “SPION concentration”) were injected into rats. Thus, this concentration corresponds to the highest SPIONs concentration found in plasma. Then we took as reference the albumin concentration in plasma (600 µM [32]) to define the lowest protein/SPIONs ratio in this study, which corresponds to a molar ratio of 0.11 (Table 1). Keeping the same protein concentration, we decreased the amount of coated SPIONs, mimicking the decrease in NP circulation *in vivo* over time [17]. To be able to compare the effect of NPs on albumin with those of the other proteins of this study (transferrin, fetuin-A, and hemoglobin), we kept the same ratios for all proteins, even though the protein/SPIONs ratios are higher than the physiological ones (Table 1).

When protein interacted with the coated SPIONs, the protein fluorescence decreased with increased NPs concentration, indicating NPs act as a quencher (Figure S4-S7). In the present study, none of the proteins induced a shift in the maximum fluorescence with the increasing concentration of NPs, showing that protein adsorption onto NPs did not lead to significant structural changes around the tryptophane residues. This is in contrast to a previous study of bovine serum albumin (BSA) adsorption onto SPIONs, which revealed a small red shift in BSA maximum emission wavelength, suggesting some structural changes [25].

Table 1. Summary of protein/NPs ratios for the fluorescence quenching study, and comparison with physiological ratios expected from the previous *in vivo* study **[17]**

	BSA/Tf/Ft (μM)	SPIONs (μM)	Hb (μM)	SPIONs (μM)	Ratio protein/SPIONs (μM/μM)
Fluorescence quenching	4.00	350	6.00	525	0.011
		300		450	0.013
		250		375	0.016
		200		300	0.020
		150		225	0.027
		100		150	0.040
	Protein	**MW (kDa)**	**Average concentration in plasma (μM)**	**SPIONs injected *in vivo* (μM)[17]**	**Ratio protein/SPIONs (μM/μM)**
Physiological concentration	Albumin	66	600 [32]	5000	0.11
	Transferrin	80	25.5 [33]		0.0051
	Hemoglobin	64.5	4.8 [34]		0.00096
	Fetuin-A	49	10.20 [35]		0.0020

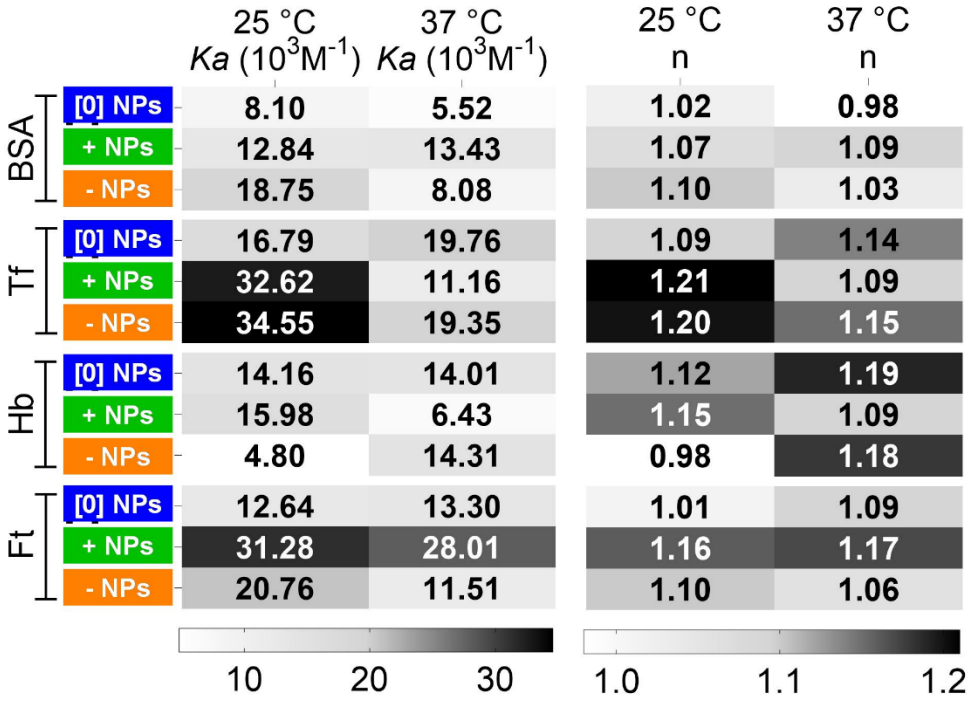

Figure 2. Binding affinity (*Ka*) and number of binding site (n) calculated for BSA (bovine serum albumin), Tf (transferrin), Hb (hemoglobin), Ft (fetuin-A), [0] NPs (neutral NPs), + NPs (positive NPs), - NPs (negative NPs) (mean values, n=3). The values were obtained by treating the fluorescence quenching data with the modified Stern-Volmer equation.

Then, we proceeded to calculate the protein binding affinity (*Ka*) and number of binding sites (*n*) by applying the modified Stern-Volmer equation [36], where F_0 and F correspond to the fluorescence intensity of protein in the absence and presence of the quenching NPs, respectively:

$$log\frac{F_0 - F}{F} = \log K_a + n\log([NPs]) \quad \text{Equation 1}$$

The results obtained for the different proteins are summarized in Figure 2 and Table S3. The first two columns show the binding affinity values at two different temperatures (25 °C and 37 °C). The highest *Ka* was found at 25 °C for both transferrin and fetuin adsorbed onto positively and negatively charged NPs. There is an overall decrease in *Ka* values at 37 °C, with the highest binding affinities corresponding to fetuin adsorbed onto positively charged NPs, similar to the behavior at 25 °C. However, transferrin has a different behavior since its interaction with positively charged NPs seems less favorable at a higher temperature, suggesting that temperature is a key factor in protein-NPs interaction, as has been mentioned by other authors [37].

As mentioned, the highest binding affinity corresponded to transferrin binding to the positively and negatively charged NPs at 25 °C, with *Ka* values around $30*10^3$ M^{-1}. These values correspond to low binding affinities, typical for non-specific interactions. In comparison, Tf binding to its receptor would lead to a much higher affinity of 10^8 M^{-1} [38]. This also explains the difficulties with the QCM experiment since the low binding affinities justify the need to apply a high NP concentration to measure protein-NPs interaction.

Following the same tendency as the binding affinity, the number of binding sites decreased with increase in temperature. The conclusions drawn from the number of binding sites need to be considered carefully. While some papers interpret *n* as the number of protein binding sites [20, 25, 39, 40], it is important to consider that *n* represents the Hill coefficient [36]. The values shown in Figure 2 indicate that the Hill coefficient varied between 0.98 and 1.21, which corresponds to no cooperativity [41], meaning that the binding of one ligand molecule does not affect the binding of adjacent molecules. In this case, the protein still might have one or multiple non-cooperative ligand-binding sites, which cannot be deduced from the data obtained [42, 43].

Finally, while QCM results suggest that protein-NPs binding is mainly electrostatically driven, this is not so clear from the analysis of the binding constants. Focusing on the data at 25 °C (the same temperature as the QCM experiment), the + NPs have the strongest interaction with Tf and Ft. Contrarily, BSA seemed to have the highest interaction with + NPs in QCM experiments. The difference in the results might be related to the technique since QCM required the previous fixation of protein onto the sensor, while fluorescence emission was measured after the protein established an equilibrium with NPs in solution. The differences in the affinity stress the need to apply orthogonal techniques to understand protein-NPs interactions better.

3.2. Secondary structure

Circular dichroism

Besides the binding affinity, it is also important to check the structural integrity of the proteins when interacting with the NPs, which can be performed applying circular dichroism (CD). This technique allowed us to assess changes in the protein structure upon interaction with the NPs in solution.

When designing the experimental conditions, the first criteria was that NP CD spectral changes would be negligible, achieved for NP concentration below 80 µM. Then, the protein concentration needed to be high enough to obtain a high-intensity spectrum, but low enough to ensure that all proteins in the solution interacted with NPs. The latter was essential to ensure that possible protein structure alterations were not masked by the spectra of free protein in solution (which would assume its native structure). Therefore, the lowest protein/NPs ratio applied for fluorescence was divided by half, meaning that protein/SPIONs solutions at a molar ratio of 0.005 were prepared.

Figure 3a shows the CD protein spectra obtained for proteins interacting with the differently charged NPs. Transferrin maintained its native structure when interacting with the different NPs, while the fetuin structure was the most affected by + NPs. On the other hand, the interaction with the three different NPs affected both Hb and BSA conformations.

Furthermore, to quantify the different types of content of secondary structures, far-UV CD spectra were analyzed by the algorithm SELCON3 [21], as shown in Figure 3b (1st column). Then, the structure variation (Δ fraction) was calculated to better understand the NPs' influence on the protein structure, as shown in Figure 3b (2nd column). BSA, Hb, and Ft structures suffered the greatest changes when interacting with the positively charged NPs. This is in agreement with the data obtained by the QCM measurements, indicating that higher affinity might be related to higher changes in the secondary structure. However, this was not the case for transferrin, which had one of the highest affinities to the NPs according to QCM and fluorescence quenching, although it did not translate into a loss of its native structure. Consequently, we may hypothesize that the Tf/NPs interaction occurs in a region that does not affect the protein structure.

A decrease in albumin’s α-helix content to values around 0.35 was previously correlated to protein denaturation [13], while an increase is linked to higher protein stability [44, 45]. Our results showed a small decrease in α-helix structure upon interaction with the different NPs, with the minimum α-helix content being registered to the BSA/+NPs interaction of around 0.6, suggesting that the studied NPs do not denature albumin in solution.

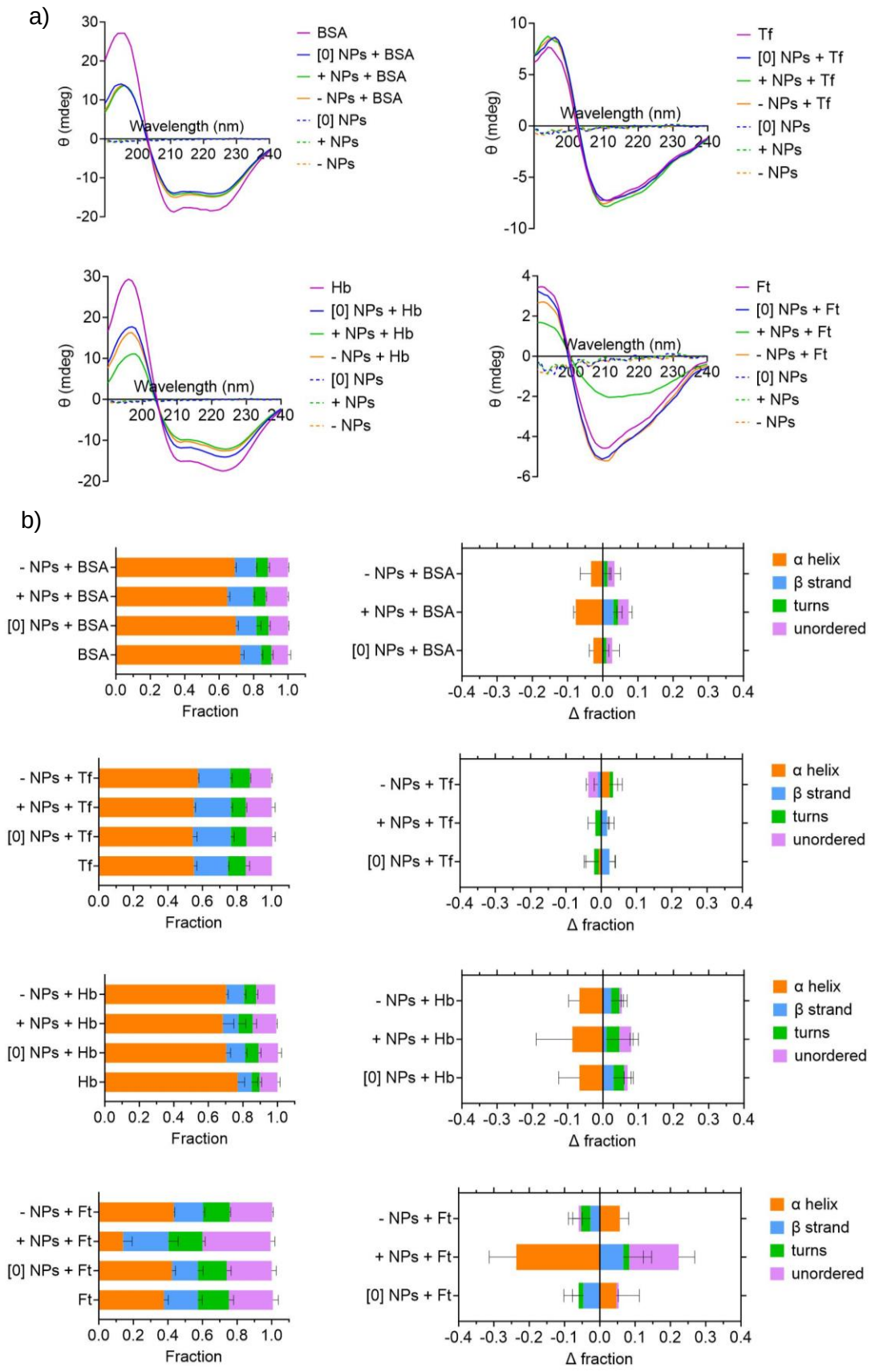

Figure 3. (a) Far-UV CD spectra of proteins alone (BSA, Tf, Hb, and Ft) and in solution in the presence of the different NPs ([0] NPs, + NPs, and – NPs), obtained at 25 °C (n=3). (b) the left graphs represent the secondary structure composition of each protein alone and during

interaction with the different NPs, while the graphs on the right represent the change in the secondary structure (Δ fraction) during interaction with NPs.

Fetuin-A is characterized by small α-helix content [30, 46]. If solubilized in a urea solution, Ft suffered an increase in random conformation, while dissolution in chloroethanol (organic solvent) increased its α-helix structure content [46]. The increase in α-helix shown for Ft/[0] NPs and Ft/- NPs interactions has been associated with an exposition of the protein's hydrophobic regions, which would also lead to a shift of the maximum of fluorescence after tryptophan excitation [30, 46]. However, the results discussed previously showed that the increase in α-helix did not change the maximum wavelength of emission (Figure S7). On the other hand, the increase in β-sheet confirmed for + NPs interaction has been associated with the formation of amyloid fibrils [47], which has been identified as a generic danger signal to the immune system [48]. However, fibril formation would have to be proven by complementary measurements, e.g., by transmission electron microscopy (TEM) [30].

Finally, hemoglobin interaction with the different NPs lead to a slight decrease in the α-helix structure, associated with its partial denaturation [49-51]. Still, it is possible to observe peaks at wavelengths around 210 nm and 220 nm for the Hb/NPs interaction spectrum (Figure 3a), which indicates that the unfolding of Hb did not achieve the hemichrome state, leading to Hb dimerization [51].

4. Overall discussion

This study aimed to investigate the interactions between different proteins (albumin, transferrin, hemoglobin, and fetuin) and NPs of different surface charges and compare the data obtained with the protein corona data obtained from an *in vivo* study performed with similar NPs [17]. QCM and fluorescence quenching explored the binding affinity, while potential changes in the secondary structure were investigated by CD.

BSA and transferrin were previously identified as part of the top 10 most abundant proteins adsorbed *in vivo* [17] independently of their charge. This can be related to the affinity of these proteins to the NP surface and their high abundance in the blood [5]. Fetuin-A, identified as one of the most abundant constituents of the hard corona [44, 52, 53], was correlated with the increase in the circulation time of [0] NPs and - NPs. Contrarily, hemoglobin, which has a low concentration in the blood (Table 1), was identified as a key protein that shortens + NPs circulation time since it was one of the most abundant components of the protein corona of these short-lived NPs [17].

Previous studies have shown that negatively charged NPs interact with Hb leading to reversible changes in its secondary structure, preserving its functionality [54]. However, Hb interaction with positively charged NPs leads to heme degradation and promotes NP aggregation [27, 55]. Thus, it was hypothesized that hemoglobin would have a high affinity to the + NPs, inducing protein structure changes and ultimately exposing new epitopes, stimulating + NPs elimination by the immune system.

Focusing on the data obtained at 25 °C, Hb showed highest binding affinity to positive NPs on both QCM and fluorescence quenching measurements, compared to [0] NPs and - NPs. Accordingly, this interaction led to the highest loss in α helix structure

(Figure 3). While the Hb/[0] NPs and Hb/- NPs interactions lead to an increase of both β-sheets and turns, Hb/+ NPs interaction lead to an increase of unordered structures. Thus, we hypothesized that this might indicate that + NPs lead to higher changes in Hb secondary structure. In order to confirm this assumption, we performed UV spectroscopy to investigate Hb degradation, since the consequent hemichrome release should lead to a shift of the maximum absorption.

The UV absorption spectra (Figure S8) showed the characteristic bands of hemoproteins, namely, the Soret band centered at 415 nm for oxy-hemoglobin [56]. The blue shift observed is associated with Hb degradation [56-58], which might indicate Hb denaturation towards hemichrome formation [57, 59]. Unfortunately, since SPIONs have a considerable UV absorbance at around 370 nm (Figure S8), it is not possible to confirm the absence of free hemin in the solution [51], as suggested by CD data. Still, the peaks between 550 nm and 650 nm did not change with the increase of coated NPs concentration, which supports the lack of free hemin formation [51, 57, 59]. Namely, it was not considered how the change in Hb structure would affect its interaction with other proteins, which reminds us that this is a simplistic modularization of the *in vivo* complexity. Still, the *in vitro* Hb-NPs interaction characterization supports our initial hypothesis that + NPs lead to higher changes in Hb structure, potentially stimulating NPs elimination.

Furthermore, this study revealed a general tendency for bigger changes in the protein structure after interacting with + NPs, which could be correlated with stronger protein-NPs interaction. Similarly, the interaction of fetuin-A with + NPs lead to a significant decrease in α helix structure (> 20 %), suggesting a significant change in the secondary structure. Even though fetuin-A had one of the highest *Ka* values with the + NPs (Figure 2), this protein was not identified as part of the most abundant proteins on the + NPs protein corona *in vivo* [17]. This might have two explanations: *i)* according to the Vroman effect [60], proteins with low affinity to the surface are replaced by proteins with higher affinity to the NP surface over time. However, since + NPs have a half-life of about 2 min [17], there is not enough time to observe the enrichment in fetuin-A in the protein corona of these NPs; *ii)* as mentioned before, the experiment ignores the contribution of protein-protein interaction, which might affect the protein corona enrichment.

Fetuin-A has been classified as both an opsonin and dysopsonin, depending on the NPs charge [61]. Since it was classified as a protein prolonging the blood circulation time of neutral and negatively charged NPs, it was assumed that fetuin-A would have to keep its native structure to act as a dysopsonin. In terms of structure, neither [0] NPs nor - NPs lead to significant changes in the protein structure, which supports that fetuin-A native structure might be essential for its dysopsonin activity. Unfortunately, the *Ka* data is not so conclusive. From the fluorescence measurements it is possible to conclude that the *Ka* determined for - NPs is higher than for [0] NPs, even though QCM data showed the opposite tendency. This discrepancy is probably related to the technical differences between the two techniques. While fetuin is fixed on a sensor for QCM measurements, the protein is free in solution during fluorescence quenching measurements, which might affect the protein-NP binding.

This paper starts by mentioning the relevance and challenges of *in vivo* vs. *in vitro* studies as well as single protein-NPs vs. all blood proteins-NPs interaction experiments. A paper discussing the *in vivo* protein corona differences between PVAL-coated SPIONs with different charges [17] was compared to the *in vitro* results obtained from selected proteins throughout this study. As mentioned above, the experiments confirmed the hypothesis established from the *in vivo* studies for the interaction between Hb and Ft with the different NPs. Namely that:

a) Hb has a higher binding affinity to + NPs, which leads to a higher increase in unordered structures, indicating that + NPs induce greater changes in Hb secondary structure. Thus, changes in Hb secondary structure potentially lead to faster elimination of + NPs by the immune system.
b) Neither [0] NPs nor - NPs lead to significant changes in the fetuin-A structure, which supports that its native structure might be essential for its dysopsonin activity.

However, while simplifying the experimental design allowed us to better understand the 1:1 protein-NP interaction, there are some limitations. To improve the accuracy of translating *in vitro* results to *in vivo* conclusions, we highlighted the importance of orthogonal techniques and complementary information on protein-NPs interaction, namely binding affinity, and effect on the secondary structure, which, taken together, demonstrated to be essential. In fact, studies have shown that protein binding affinity to NPs is not directly correlated with the protein concentration in the protein corona [24, 53]. This can be explained by:

a) The difficulty in considering all the physiological factors influencing protein binding affinity in the studies (media, pressure, blood flow, other proteins, etc.).
b) Protein-protein contribution to the protein corona composition and protein binding affinity
    i. Protein adsorbed into the surface might lead to the enrichment of certain proteins with which they have a higher affinity.
    ii. Protein adsorption and alteration to its structure might expose new epitopes with higher affinity to certain proteins.

Thus, affinity studies alone are not enough to predict the protein corona formation, but it is important to include other tests, such as the effect on the protein structure and influence on cell uptake. To get the full picture, it will be important to complement the results obtained in this paper with uptake studies after NPs were coated with the different proteins studied.

5. Conclusions

This comprehensive study thoroughly investigated the interactions between key proteins (albumin, transferrin, hemoglobin, and fetuin-A) and nanoparticles of different surface charges (neutral, positive, and negative) using QCM, fluorescence quenching, and circular dichroism. Hb and Ft were previously found to be important components

of the protein corona for NPs of different charges, affecting their circulation time *in vivo*.

The results could be correlated with the *in vivo* protein corona studied previously. Namely, the Hb structure changed the most with interaction with positive NPs, while the Ft structure did not suffer significant changes when in contact with [0] NPs and -NPs. Overall, data indicate that protein-NPs interactions are primarily driven by electrostatic interactions and that it is important to check for changes in the native structure since high *Ka* values do not directly translate into higher structural changes.

While the combination of binding affinity and protein structure study was essential to understand protein-NP interactions, complementary cell uptake studies would be important to unveil, for example, the effect on macrophage uptake.

Still, *in vitro* and single protein-NPs studies proved successful in obtaining direct results that can be translated into *in vivo* studies. The established *in vivo-in vitro* correlation opens new and exciting possibilities for future studies on the protein corona.

Conflict of interest

The authors declare no competing financial interest.

Author contributions

Conceptualization, C.M., G.B. and O.J.; methodology, C.M., P.M., G.B. and O.J.; validation, C.M., P.M., L.M., G.B. and O.J.; formal analysis, C.M.; investigation, C.M.; resources, L.M., G.B. and O.J.; data curation, C.M.; writing—original draft preparation, C.M.; writing—review and editing, C.M., P.M., L.M., G.B. and O.J.; visualization, C.M.; supervision, G.B. and O.J.; project administration, C.M., G.B. and O.J.; and funding acquisition, L.M., G.B. and O.J. All authors have read and agreed to the published version of the manuscript.

Acknowledgements

Authors also would like to acknowledge the supports of EIPHI Graduate School (contract ANR-17-EURE-0002) and the ANR Nanoblorona (contract ANR-21-CE18-0015).

6. References

[1] T. Lima, K. Bernfur, M. Vilanova, T. Cedervall, Understanding the Lipid and Protein Corona Formation on Different Sized Polymeric Nanoparticles, Scientific Reports 10(1) (2020) 1129.
[2] K. Anand, R. Rajamanikandan, A. Selva Sharma, M. Ilanchelian, F.I. Khan, C. Tiloke, N.K. Katari, P. Boomi, C. Balakumar, M. Saravanan, S. Palanisamy, M. Ramesh, D. Lai, A.A. Chuturgoon, Human serum albumin interaction, in silico and anticancer evaluation of Pine-Gold nanoparticles, Process Biochemistry 89 (2020) 98-109.
[3] J.E. Gagner, M.D. Lopez, J.S. Dordick, R.W. Siegel, Effect of gold nanoparticle morphology on adsorbed protein structure and function, Biomaterials 32(29) (2011) 7241-7252.
[4] M. Falahati, F. Attar, M. Sharifi, T. Haertlé, J.-F. Berret, R.H. Khan, A.A. Saboury, A health concern regarding the protein corona, aggregation and disaggregation, Biochimica et Biophysica Acta (BBA) - General Subjects 1863(5) (2019) 971-991.
[5] Q. Xiao, M. Zoulikha, M. Qiu, C. Teng, C. Lin, X. Li, M.A. Sallam, Q. Xu, W. He, The effects of protein corona on in vivo fate of nanocarriers, Advanced Drug Delivery Reviews 186 (2022) 114356.
[6] M. Mahmoudi, The need for improved methodology in protein corona analysis, Nature Communications 13(1) (2022) 49.
[7] I. Yadav, V.K. Aswal, J. Kohlbrecher, Size-dependent interaction of silica nanoparticles with lysozyme and bovine serum albumin proteins, Physical Review E 93(5) (2016) 052601.
[8] M. Lundqvist, J. Stigler, G. Elia, I. Lynch, T. Cedervall, K.A. Dawson, Nanoparticle size and surface properties determine the protein corona with possible implications for biological impacts, Proceedings of the National Academy of Sciences 105(38) (2008) 14265-14270.
[9] K. Giri, I. Kuschnerus, M. Lau, J. Ruan, A. Garcia-Bennett, Pore structure and particle shape modulates the protein corona of mesoporous silica particles, Materials Advances 1(4) (2020) 599-603.
[10] M.P. Vincent, N.B. Karabin, S.D. Allen, S. Bobbala, M.A. Frey, S. Yi, Y. Yang, E.A. Scott, The Combination of Morphology and Surface Chemistry Defines the Immunological Identity of Nanocarriers in Human Blood, Advanced Therapeutics 4(8) (2021) 2100062.
[11] A. Nandakumar, W. Wei, G. Siddiqui, H. Tang, Y. Li, A. Kakinen, X. Wan, K. Koppel, S. Lin, T.P. Davis, D.T. Leong, D.J. Creek, F. Ding, Y. Song, P.C. Ke, Dynamic Protein Corona of Gold Nanoparticles with an Evolving Morphology, ACS applied materials & interfaces 13(48) (2021) 58238-58251.
[12] M. Kokkinopoulou, J. Simon, K. Landfester, V. Mailänder, I. Lieberwirth, Visualization of the protein corona: towards a biomolecular understanding of nanoparticle-cell-interactions, Nanoscale 9(25) (2017) 8858-8870.
[13] M.P. Vincent, S. Bobbala, N.B. Karabin, M. Frey, Y. Liu, J.O. Navidzadeh, T. Stack, E.A. Scott, Surface chemistry-mediated modulation of adsorbed albumin folding state specifies nanocarrier clearance by distinct macrophage subsets, Nature Communications 12(1) (2021) 648.
[14] N. Bertrand, P. Grenier, M. Mahmoudi, E.M. Lima, E.A. Appel, F. Dormont, J.-M. Lim, R. Karnik, R. Langer, O.C. Farokhzad, Mechanistic understanding of in vivo protein corona formation on polymeric nanoparticles and impact on pharmacokinetics, Nature Communications 8(1) (2017) 777.
[15] M.J. Hajipour, H. Aghaverdi, V. Serpooshan, H. Vali, S. Sheibani, M. Mahmoudi, Sex as an important factor in nanomedicine, Nature Communications 12(1) (2021) 2984.
[16] Y. Liu, J. Wang, Q. Xiong, D. Hornburg, W. Tao, O.C. Farokhzad, Nano–Bio Interactions in Cancer: From Therapeutics Delivery to Early Detection, Accounts of chemical research 54(2) (2021) 291-301.
[17] C. Marques, M.J. Hajipour, C. Marets, A. Oudot, R. Safavi-sohi, M. Guillemin, G. Borchard, O. Jordan, L. Saviot, L. Maurizi, Identification of the Proteins Determining the Blood Circulation Time of Nanoparticles, ACS nano (2023).
[18] C. Marques, L. Maurizi, G. Borchard, O. Jordan, Characterization Challenges of Self-Assembled Polymer-SPIONs Nanoparticles: Benefits of Orthogonal Methods, Int J Mol Sci 23(24) (2022).
[19] F. Höök, Development of a novel QCM technique for protein adsorption studies: Department of Biochemistry and Biophysics and Department of Applied Physics, Chalmers University of Technology, Chalmers University of Technology, Götebory University: Göteborg, Sweden (1997) 60.

[20] F.C. Santos, P.J. Costa, M.H. Garcia, T.S. Morais, Binding of RuCp complexes with human apo-transferrin: fluorescence spectroscopy and molecular docking methods, BioMetals 34(5) (2021) 1029-1042.
[21] L. Whitmore, B.A. Wallace, DICHROWEB, an online server for protein secondary structure analyses from circular dichroism spectroscopic data, Nucleic Acids Research 32(suppl_2) (2004) W668-W673.
[22] U. Kragh-Hansen, Structure and ligand binding properties of human serum albumin, Dan Med Bull 37(1) (1990) 57-84.
[23] M.Y. Rosseneu-motreff, F. Soetewey, R. Lamote, H. Peeters, Size and shape determination of apotransferrin and transferrin monomers, Biopolymers 10(6) (1971) 1039-1048.
[24] H. Moustaoui, J. Saber, I. Djeddi, Q. Liu, D. Movia, A. Prina-Mello, J. Spadavecchia, M. Lamy de la Chapelle, N. Djaker, A protein corona study by scattering correlation spectroscopy: a comparative study between spherical and urchin-shaped gold nanoparticles, Nanoscale 11(8) (2019) 3665-3673.
[25] S. Yu, A. Perálvarez-Marín, C. Minelli, J. Faraudo, A. Roig, A. Laromaine, Albumin-coated SPIONs: an experimental and theoretical evaluation of protein conformation, binding affinity and competition with serum proteins, Nanoscale 8(30) (2016) 14393-14405.
[26] W. Wang, Z. Zhong, Z. Huang, F. Fu, W. Wang, L. Wu, Y. Huang, C. Wu, X. Pan, Two different protein corona formation modes on Soluplus® nanomicelles, Colloids and Surfaces B: Biointerfaces 218 (2022) 112744.
[27] H. Yang, C. Hao, Z. Nan, R. Sun, Bovine hemoglobin adsorption onto modified silica nanoparticles: Multi-spectroscopic measurements based on kinetics and protein conformation, International Journal of Biological Macromolecules 155 (2020) 208-215.
[28] J.R. Lakowicz, Principles of fluorescence spectroscopy, Springer2006.
[29] C. Wang, I. Lascu, A. Giartosio, Bovine Serum Fetuin Is Unfolded through a Molten Globule State, Biochemistry 37(23) (1998) 8457-8464.
[30] N. Zaidi, S. Nusrat, F.K. Zaidi, R.H. Khan, pH-Dependent Differential Interacting Mechanisms of Sodium Dodecyl Sulfate with Bovine Serum Fetuin: A Biophysical Insight, The Journal of Physical Chemistry B 118(46) (2014) 13025-13036.
[31] D. Wrobel, M. Marcinkowska, A. Janaszewska, D. Appelhans, B. Voit, B. Klajnert-Maculewicz, M. Bryszewska, M. Štofik, R. Herma, P. Duchnowicz, J. Maly, Influence of core and maltose surface modification of PEIs on their interaction with plasma proteins—Human serum albumin and lysozyme, Colloids and Surfaces B: Biointerfaces 152 (2017) 18-28.
[32] T. Peters, Serum Albumin, in: C.B. Anfinsen, J.T. Edsall, F.M. Richards (Eds.), Advances in Protein Chemistry, Academic Press1985, pp. 161-245.
[33] A.S. Ogun, A. Adeyinka, Biochemistry, Transferrin, StatPearls Publishing, Treasure Island (FL)2022.
[34] H. Chaplin, M. Cassell, G. Hanks, The stability op the plasma hemoglobin level in the normal human subject, The Journal of Laboratory and Clinical Medicine 57(4) (1961) 612-619.
[35] W. Brown, K. Dziegielewska, N. Saunders, K. Møsllgård, Fetuin-an old friend revisited, Bioessays 14(11) (1992) 749-755.
[36] K.A. Bakar, S.R. Feroz, A critical view on the analysis of fluorescence quenching data for determining ligand–protein binding affinity, Spectrochimica Acta Part A: Molecular and Biomolecular Spectroscopy 223 (2019) 117337.
[37] M. Mahmoudi, A.M. Abdelmonem, S. Behzadi, J.H. Clement, S. Dutz, M.R. Ejtehadi, R. Hartmann, K. Kantner, U. Linne, P. Maffre, S. Metzler, M.K. Moghadam, C. Pfeiffer, M. Rezaei, P. Ruiz-Lozano, V. Serpooshan, M.A. Shokrgozar, G.U. Nienhaus, W.J. Parak, Temperature: The "Ignored" Factor at the NanoBio Interface, ACS nano 7(8) (2013) 6555-6562.
[38] J. Schüler, J. Frank, U. Trier, M. Schäfer-Korting, W. Saenger, Interaction Kinetics of Tetramethylrhodamine Transferrin with Human Transferrin Receptor Studied by Fluorescence Correlation Spectroscopy, Biochemistry 38(26) (1999) 8402-8408.

[39] Z. Chi, R. Liu, Y. Teng, X. Fang, C. Gao, Binding of Oxytetracycline to Bovine Serum Albumin: Spectroscopic and Molecular Modeling Investigations, Journal of Agricultural and Food Chemistry 58(18) (2010) 10262-10269.
[40] N. Wang, L. Ye, F. Yan, R. Xu, Spectroscopic studies on the interaction of azelnidipine with bovine serum albumin, International journal of pharmaceutics 351(1) (2008) 55-60.
[41] Z. Grabarek, J. Gergely, Appendix. On the applicability of Hill type analysis to fluorescence data, Journal of Biological Chemistry 258(23) (1983) 14103-14105.
[42] D.I. Cattoni, O. Chara, S.B. Kaufman, F.L. González Flecha, Cooperativity in Binding Processes: New Insights from Phenomenological Modeling, PLOS ONE 10(12) (2016) e0146043.
[43] M. van de Weert, L. Stella, Fluorescence quenching and ligand binding: A critical discussion of a popular methodology, Journal of Molecular Structure 998(1) (2011) 144-150.
[44] W. Lai, D. Li, Q. Wang, X. Nan, Z. Xiang, Y. Ma, Y. Liu, J. Chen, J. Tian, Q. Fang, A Protein Corona Adsorbed to a Bacterial Magnetosome Affects Its Cellular Uptake, International Journal of Nanomedicine 15 (2020) 1481-1498.
[45] H. Yang, M. Wang, Y. Zhang, F. Li, S. Yu, L. Zhu, Y. Guo, L. Yang, S. Yang, Conformational-transited protein corona regulated cell-membrane penetration and induced cytotoxicity of ultrasmall Au nanoparticles, RSC Advances 9(8) (2019) 4435-4444.
[46] F. Gejyo, J.L. Chang, W. Bürgi, K. Schmid, G.D. Offner, R.F. Troxler, H. Van Halbeek, L. Dorland, G.J. Gerwig, J.F. Vliegenthart, Characterization of the B-chain of human plasma alpha 2HS-glycoprotein. The complete amino acid sequence and primary structure of its heteroglycan, Journal of Biological Chemistry 258(8) (1983) 4966-4971.
[47] R. Nelson, D. Eisenberg, Structural Models of Amyloid-Like Fibrils, Advances in Protein Chemistry, Academic Press2006, pp. 235-282.
[48] A. Gustot, V. Raussens, M. Dehousse, M. Dumoulin, C.E. Bryant, J.-M. Ruysschaert, C. Lonez, Activation of innate immunity by lysozyme fibrils is critically dependent on cross-β sheet structure, Cellular and Molecular Life Sciences 70(16) (2013) 2999-3012.
[49] A. Ikai, H. Noda, Partially Helical Conformation of Hemoglobin in Aqueous 2-Chloroethanol, Journal of Biological Chemistry 243(19) (1968) 5028-5034.
[50] R. Mondal, N. Ghosh, S. Mukherjee, Contrasting effects of pH on the modulation of the structural integrity of hemoglobin induced by sodium deoxycholate, Physical Chemistry Chemical Physics 18(44) (2016) 30867-30876.
[51] L. Fotouhi, S. Yousefinejad, N. Salehi, A.A. Saboury, N. Sheibani, A.A. Moosavi-Movahedi, Application of merged spectroscopic data combined with chemometric analysis for resolution of hemoglobin intermediates during chemical unfolding, Spectrochimica Acta Part A: Molecular and Biomolecular Spectroscopy 136 (2015) 1974-1981.
[52] H. Mohammad-Beigi, Y. Hayashi, C.M. Zeuthen, H. Eskandari, C. Scavenius, K. Juul-Madsen, T. Vorup-Jensen, J.J. Enghild, D.S. Sutherland, Mapping and identification of soft corona proteins at nanoparticles and their impact on cellular association, Nature Communications 11(1) (2020) 4535.
[53] R.L. Pinals, D. Yang, D.J. Rosenberg, T. Chaudhary, A.R. Crothers, A.T. Iavarone, M. Hammel, M.P. Landry, Quantitative Protein Corona Composition and Dynamics on Carbon Nanotubes in Biological Environments, Angewandte Chemie International Edition 59(52) (2020) 23668-23677.
[54] S. Devineau, L. Zargarian, J.P. Renault, S. Pin, Structure and Function of Adsorbed Hemoglobin on Silica Nanoparticles: Relationship between the Adsorption Process and the Oxygen Binding Properties, Langmuir 33(13) (2017) 3241-3252.
[55] S.Y. Mobasherat Jajroud, M. Falahati, F. Attar, R.A. Khavari-Nejad, Human hemoglobin adsorption onto colloidal cerium oxide nanoparticles: a new model based on zeta potential and spectroscopy measurements, Journal of Biomolecular Structure and Dynamics 36(11) (2018) 2908-2916.
[56] J.W.P. Carvalho, F.A.O. Carvalho, P.S. Santiago, M. Tabak, Thermal denaturation and aggregation of hemoglobin of Glossoscolex paulistus in acid and neutral media, International Journal of Biological Macromolecules 54 (2013) 109-118.

[57] P.P. Samuel, M.A. White, W.C. Ou, D.A. Case, G.N. Phillips, J.S. Olson, The Interplay between Molten Globules and Heme Disassociation Defines Human Hemoglobin Disassembly, Biophysical Journal 118(6) (2020) 1381-1400.
[58] E.K. Hanson, J. Ballantyne, A Blue Spectral Shift of the Hemoglobin Soret Band Correlates with the Age (Time Since Deposition) of Dried Bloodstains, PLOS ONE 5(9) (2010) e12830.
[59] W. Liu, X. Guo, R. Guo, The interaction between hemoglobin and two surfactants with different charges, International Journal of Biological Macromolecules 41(5) (2007) 548-557.
[60] L. Vroman, A.L. Adams, Identification of rapid changes at plasma–solid interfaces, Journal of Biomedical Materials Research 3(1) (1969) 43-67.
[61] L. Thiele, J.E. Diederichs, R. Reszka, H.P. Merkle, E. Walter, Competitive adsorption of serum proteins at microparticles affects phagocytosis by dendritic cells, Biomaterials 24(8) (2003) 1409-1418.